J Micro-Bio Robot (2013) 8:41–52
DOI 10.1007/s12213-012-0054-0

REVIEW PAPER

Microrobotics in the vascular network: present status and next challenges

Sylvain Martel

Received: 29 February 2012 / Revised: 1 October 2012 / Accepted: 29 October 2012 / Published online: 26 January 2013

Abstract The field of microrobotics dedicated to medical interventions although relatively new, is progressing at a very fast pace. Among the various accesses inside the body being investigated, the vascular network with close to 100,000 km of potential routes in each human and offering a large range of interventional opportunities has been of special interest in recent years. Although significant progresses and milestones have been achieved in this particular field of research, some important challenges remain to be solved before microrobotics in the human vasculature becomes a reality. Nonetheless, despite these challenges, some applications are already on the horizon. This paper aims at providing a quick overview of the present status of the field of microrobotics for interventions in the vascular network and to describe the main critical challenges that must be met in the short term to enable new or enhanced medical interventional procedures that may bring potential great outcomes for the patients.

Keywords Medical imaging modalities · Targeted interventions · magnetic nanoparticles · vascular network · medical microrobotics

1 Introduction

In the field of microrobotics, several recent papers have presented theoretical formulations with simulated or experimental data where the authors claim that the results could potentially be applied in the human vascular network. Although of great scientific values, in many instances, the results concern only the controlled displacement of a small untethered object using an experimental setup that often failed to take into account all the main critical physiological, technological, and medical constraints.

As a simple example, besides the lack of information about the possibility of scaling many of these relatively small experimental apparatus at the human scale, in these papers and related experiments, optical microscopy is most often used to gather the position of the micro-object (often referred to as a microrobot) required to compute the corrective actions using a given real-time control algorithm. But such imaging modality cannot be applied when performing closed-loop navigation control in the vascular network. Instead, other imaging modalities need to be considered. These imaging modalities can add substantial constraints such as latency in the control loop that can often be beyond a threshold that would fail to guarantee robustness, while lacking sufficient spatial resolution for tracking microscale devices or robots. Only one of these two examples among a longer list of possible variables would often be sufficient to impose critical constraints that would prevent the applicability of the technique for operations intended to be conducted in the vascular network.

As such, a system-oriented approach within the required interdisciplinary research environment instead a single discipline-oriented research strategy is a must for the successful implementation of microrobotic methods in this particular research area. Indeed, the main challenge is to expand the knowledge and to interact successfully beyond a particular field of specialization in order to identify and predict potential technical challenges ahead of time such that proper research and development efforts could be initiated.

Therefore, the goal of this paper is not only to provide the present status and to give a feel about the

S. Martel (✉)
NanoRobotics Laboratory, Department of Computer and Software Engineering, and Institute of Biomedical Engineering,
École Polytechnique de Montréal (EPM),
Campus of the Université de Montréal,
Montréal, Canada
e-mail: sylvain.martel@polymtl.ca

interdisciplinary nature of this particular field of microrobotics but also to provide information about the most critical constraints that must be taken into account in future research and development efforts. Such constraints are in great part responsible for the identification of the next critical challenges that are described in this paper in an effort to guide future research initiatives in this promising and exciting field of robotics.

2 Initial implementations

Medical microrobotics can fall onto one of two main categories that could be identified as fully-autonomous or assisted where the latter would include semi- or partially-autonomous, and non-autonomous. The well publicized portrait of microrobots navigating in the blood vessels to repair organs, remove plaque, or other tasks performed without external help is an example that could be categorized as fully-autonomous. Although this could be envisioned in a relatively far future, with present technological constraints in mind, fully-autonomous applications or implementations are unlikely for awhile, at least in the short term. As such and in light of the level of complexity already present and briefly described in this paper for non fully-autonomous implementations, it becomes evident that the initial medical interventions to be successful and reliable would and should be assisted by external hardware and software.

Such assisted interventions should begin with the most fundamental task which is the controlled displacements in the vascular network of relatively simple microscale entities designed for a particular task (referred to here as navigable agents) towards regions typically inaccessible to catheterization. The control offered by such microrobotic component would allow the user to avoid systemic circulation while reducing travel time. As such, displacements of such agents would typically be done following a pre-determined path or trajectory for targeted imaging, sensory/diagnostic, surgical, and/or therapeutic applications.

In order to increase the likelihood of making such new technology accessible for the patients in the shorter term, applications aimed at specific cases where all medical interventions have failed a priori and where microrobotics can provide valuable solutions are most likely to succeed as new interventional tools in future clinical practices. But the choice of such interventions will dictate an appropriate design for the microrobotic platform and the related navigable agents. Therefore, the most fundamental aspects for the implementation of such microrobotic platforms and related navigable agents need to be taken into account. These fundamental aspects identified in this paper are primarily related to imaging and actuation issues.

3 Imaging

Considering the absence of direct line-of-sight and the limited spatial resolution of existing medical imaging modalities, the imaging aspect including the tracking of such agents navigating along pre-determined paths is certainly one of the most critical aspects that would pose real challenges for microrobotics being performed in the vascular network.

For microrobotic-based interventions, medical imaging can fall into three categories namely, pre-operative, intra-operative, and post-operative. Pre-operative imaging involves the gathering of physiological data such as the location of the targeted site (e.g., a tumor), and images of the blood vessels necessary for determining the reference trajectory or path to be used during the navigation phase (as part of the intra-operative). Post-operative imaging would generally be used to verify the work done such as assessing the targeting efficacy in terms of quantity and distribution of navigable agents in the targeted area during drug delivery applications for instance. Longer term post-operative imaging could also be performed to assess the longer term impact of the work done. Assessing the therapeutic efficacy such as monitoring tumor regressions is one example.

Because of the real-time requirement, the intra-operative phase may represent the greater challenge for imaging or tracking during microrobotic interventions. As such, the choice of a proper medical imaging modality becomes critical for the success of the intervention.

3.1 Intra-operative phase

Practically, the choice of an adequate clinical imaging modality for microrobotic-based interventions in the vascular network is limited to ultrasound (US), Positron Emission Tomography (PET), x-ray or Computed Tomography (CT) including fluoroscopy, and Magnetic Resonance Imaging (MRI). Although being substantially less expensive than other imaging modalities, the signal-to-noise ratio (SNR) of US is far from adequate to detect microscale navigable agents. For PET, the navigable agents would have to be labeled with radioisotopes which put constraints on the number of interventions that can be done for the same patient within a specific time interval while the relatively short active period of isotopes (up to a few hours) put severe time limitations on the whole interventional procedure. Although the sensitivity of PET to detect microscale agents properly labeled is superior to any other imaging modalities, the spatial resolution compared to CT and MRI is much less. Furthermore, a PET scan takes relatively much longer time than a CT scan which puts an additional constraint to achieve real-time performance during the intra-operative phase. The overall real-time performance of CT is generally superior compared to PET or MRI for

microrobotic-based interventions. CT has also a slightly better spatial resolution than MRI but still insufficient to detect agents navigable past the arteries.

Indeed, although arteries have diameters up to a few millimeters, the arterioles connecting to arteries have diameters ranging from a few tens of micrometers (μm) up to approximately 150 μm, limiting the use of CT as an imaging modality for interventions in the arteries only. With recent catheterization techniques capable of operating within vessel's diameters of slightly less than 1 mm, navigation of untethered agents using CT as an imaging modality may be feasible and mostly advantageous in complex vascular regions delimited with diameters ranging from less than 1 mm down to ~200 μm which corresponds to the best spatial resolution achievable with CT. As mentioned earlier, this is practically insufficient to reach the arterioles and for some applications such as in cancer therapy [1, 2], it is still too far away from tumors to achieve substantially better therapeutic effects compared to presently known techniques.

Although typically MRI has a slightly lower spatial resolution than CT, unlike any other imaging modalities, an untethered microscale agent much smaller than a single voxel (3D pixel) can be synthesized to generate a signature or pattern larger than the agent itself [3] and sufficiently large to be detected by MRI, i.e., visualization through susceptibility artifacts [4]. For instance, magnetic material embedded in a navigable therapeutic agent can induce a field distortion (perturbation) similar to a magnetic dipole. Such local magnetic field distortion can be estimated at a point P of coordinate r (x, y, z) by that of a magnetic dipole as

$$\vec{B}'(P) = \frac{\mu_0}{4\pi}\left(3\frac{(\vec{m}.\vec{r})\vec{r}}{r^5} - \frac{\vec{m}}{r^3}\right) \quad (1)$$

where $\mu_0 = 4\pi \cdot 10^{-7}\,\mathrm{H \cdot m^{-1}}$ is the permeability of free space with the magnetic moment $\boldsymbol{m}$ being generally defined as

$$\vec{m} = \frac{V_P \Delta\chi \vec{B}}{\mu_0} \quad (2)$$

In Eq. 2, V_P is the volume of the magnetic particle, $\Delta\chi$ is the magnetic susceptibility difference between the magnetic material and its surrounding fluid or environment, and $\boldsymbol{B}$ is the magnetic field strength typically from a 1.5 Tesla (T) or 3 T clinical MRI scanner.

Although it was shown that a single magnetic agent with an overall diameter as small as 15 μm can be detected with a 1.5 T clinical scanner [5] by generating a dipole of sufficient intensity for the sensitivity of the scanner at the edges of a voxel with a size of $\sim 0.5 \times 0.5 \times 0.5\ \mathrm{mm}^3$, real-time performance for navigation purpose remains a critical issue.

For instance, in the first in vivo demonstration of an untethered object being navigated in a blood vessel using closed-loop control [6], a clinical MRI scanner was used. Because of the excessive time to acquire a whole MR-image, preventing real-time performance, a special MR-tracking method known as Magnetic Signature Selective Excitation Tracking (MS-SET) [7] was developed. MS-SET proved to be capable of detecting the position from the artifact generated (such as the one depicted in Fig. 1a) of a 1.5 mm (already below the spatial resolution of PET) ferromagnetic bead navigating under closed-loop computer navigation control in the carotid artery of a living swine. The bead had an average velocity of 10 $\mathrm{cm\,s^{-1}}$ and real-time tracking was successful as depicted in Fig. 1b where an icon was used to indicate the calculated real-time position of the bead during closed-loop navigation control. Feedback positional data were gathered between 20 and 30 times per second which proved to be adequate for real-time navigation in the artery.

But reducing further the diameter of the bead has shown to have a profound impact on the sampling rate. For instance, decreasing the overall diameter of the bead from 1.5 mm down to 0.9 mm resulted in being able to gather the position of the bead only approximately 3 times per second using a 1.5 T clinical MRI scanner. With a blood flow velocity that can reach ~0.3 $\mathrm{m\,s^{-1}}$ in the artery, this result corresponds to approximately 370 times the diameter of the bead itself per second. Considering the physiological environment such as the distances between successive vessel bifurcations or branches, this rate could represent a major constraint. In this particular case, MS-SET relied on Spin Echo (SE) MRI sequences instead of Gradient Echo (GRE) used for the 1.5 mm bead since the intensity of the distortion produced by the 0.9 mm bead was less intense and hence would have required much longer integration time during the acquisition. One way to increase the sampling rate for SE-based MS-SET sequences would be to reduce the flip angle but this would reduce the intensity of the signal as well as making detection more difficult while requiring an extension of the acquisition time.

Not for a single agent but a relatively large bolus of much smaller navigable agents as depicted in Fig. 1c, each agent with a diameter of 50 μm, MRI-based tracking requires approximately 3 s. This acquisition time can still represent a significant constraint in particular applications and particularly if closed-loop navigation control must be performed in more complex vascular networks characterized by a larger number of vessel bifurcations separated by shorter distances. In such a case and if possible, reducing the blood flow velocity to lower the travel speed of the agents could be an alternative to achieve robustness in closed-loop navigation control if extending the time of the intervention is not a major issue.

But for a typical dose of therapeutics such as Doxorubicin (DOX) being required to treat liver tumor in human for example, a relatively large number of navigable agents such as Therapeutic Magnetic Micro Carriers (TMMCs) [8] may

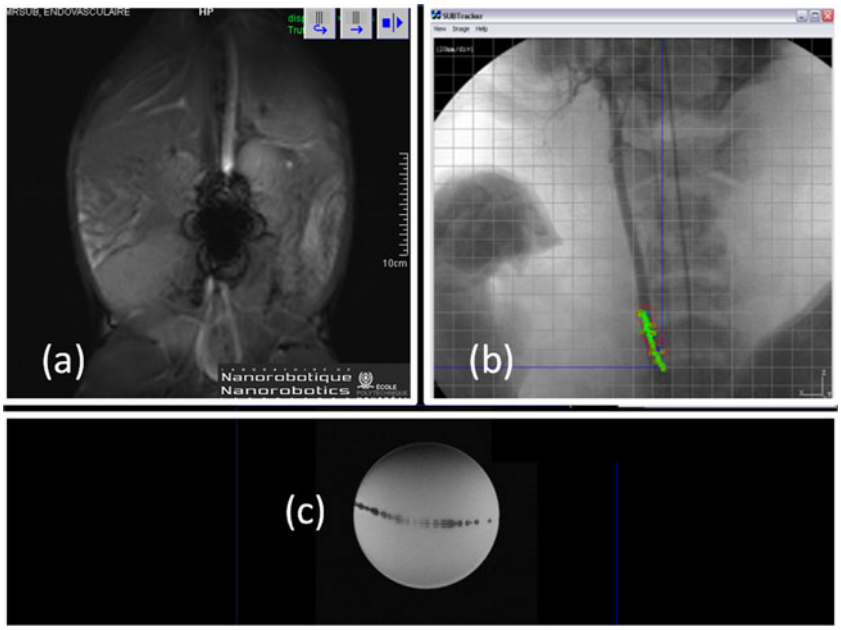

Fig. 1 **a** Example of an artifact generated by a ferromagnetic object as detected by a 1.5 T clinical MRI scanner; **b** Real-time (24 Hz) MR-tracking of a 1.5 mm ferromagnetic bead under closed-loop MR-navigation (MRN) control in the carotid artery of a living animal [6]. The position of the bead is represented by an icon after being processed from the artifact using MS-SET. In this particular case, although not essential, the position obtained with MRI has been superposed on a pre-acquired x-ray image of the animal; **c** Example of a relatively large bolus in motion of 50 μm ferromagnetic particles being detected by a 1.5 T clinical MRI scanner at every 3 s interval

be required per intervention. This number would be far too high for a single bolus considering the physiological features of the vascular network and therefore, several fast successive injections would typically be necessary. Assuming from preliminary experimental data [8] conducted in vivo, a travel time to the target of only a few seconds and the maximum overall size of each aggregate that can be directed in the appropriate branch at a vessel bifurcation [9, 10], reducing the blood flow could extend substantially the time required to conduct each intervention. Besides interventional issues and potential risks, such approach would inevitably potentially lead to a significant cost increase per intervention which may prevent or at least slow considerably the adoption of such approach in the medical community.

One alternative to speed up the process at the cost of increasing the risk of not reaching a pre-defined target is to perform navigation without or with minimum feedback tracking data during travel and to confirm the navigation path by assessing the targeting efficacy by monitoring the final position of a few agents. This approach could be used for even smaller agents.

For instance, a few minutes were required with a GRE scan on a 1.5 T clinical scanner to detect a single 15 μm magnetic bead [4] and the imaging in the liver of live rabbits of a bolus of approximately ten 50 μm in diameter of the first navigable therapeutic microcarriers being reported and known as TMMCs [8] where the initial version contained an anticancer therapeutic agent (Doxorubicin) with 40 %(*w*/*w*) ~200 nanometers (nm) FeCo magnetic nanoparticles (MNPs), each MNP being covered with a ~10 nm graphite shell, also required several minutes. The result is depicted in Fig. 2. Although this is very acceptable for assessing targeting efficacy in terms of quantity and distribution of navigable therapeutic agents during the post-operative phase, it is far from adequate for real-time closed-loop navigation control.

Besides the development of new MRI sequences, multimodal imaging could also be investigated further. For instance, PET-CT [11] and PET-MRI [12–14] are now possible but CT-MRI although possible in a XMR suite [15], cannot be used simultaneously during closed-loop navigation control. Other avenues are possible but at the present time, improving real-time performance for tracking such navigable agents is certainly one of the critical challenges requiring further investigations in the short term.

The level of improvement in this area would determine how much prediction in navigation control algorithms [16] would be required for successful targeting. Although such predictive algorithms may compensate in part for the lack of sufficient sampling rates, the approach has limitations which may inevitably result in less targeting and therapeutic efficacy and hence, higher systemic toxicity. But if the agents are made large enough to restrict interventions in the arteries only, then the spatial resolution of x-ray or CT as an imaging modality may prove to be adequate while providing the relatively fast real-time performance required for particular closed-loop control algorithms. Table 1 summarizes the advantages and limitations (described using with an arbitrary relative scaling) of each of the fundamental medical imaging modalities that can be used during microrobotic-based intra-operative interventions in the vascular network.

As depicted in Table 1, both US and x-ray provide fast real-time (RT) tracking of navigable agents. But for smaller agents down to approximately 200 μm, x-ray would typically be more appropriate. Although the real-time tracking performance of MRI which depends also on the overall size

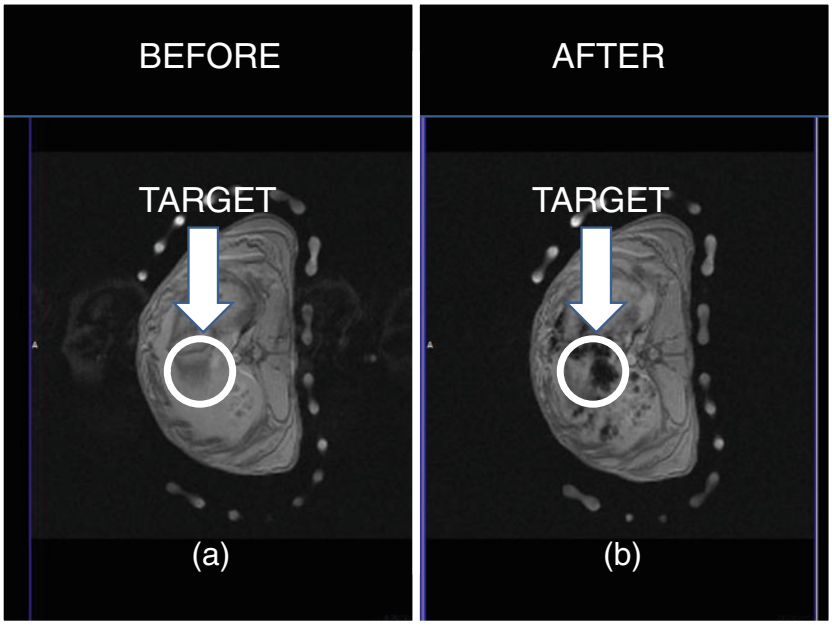

Fig. 2 MR-image obtained of a live rabbit liver before **a** and after **b** using a 1.5 T clinical MRI scanner where approximately 10 TMMCs (each with a diameter of approx. 50 μm) can be detected as a black spot in the pre-defined targeted lobe after MR-navigation being performed in the hepatic artery at 10 cm below the skin [8]

of the agents is inferior to x-ray, MRI provides the possibility of tracking agents with an overall size smaller than 200 μm if such agents are synthesized adequately. But this is done at the cost of a reduction of the real-time tracking performance. Furthermore, although the spatial resolution (Res.) of MRI is slightly lower than the one for x-ray, MRI provides high tissue contrast unlike x-ray. As such, x-ray requires several injections of contrast agents in the blood vessels for image registration purpose in order to maintain an adequate accuracy when operating in the vascular network. MRI can also use contrast agents but the image of near organs, tumors, etc., can be used also to improve the registration process although compared to x-ray, such registration typically takes more time to complete, i.e., not being performed in real-time. Multimodal imaging such as combining x-ray and MRI for registration and navigation purposes can be done, but moving the patient between the two platforms brings the risk of a potential increase in registration error. X-ray and PET are also invasive (Inv. in Table 1) for the patient which may be a factor in some cases for selecting the imaging modality used during microrobotic-based interventions. Although MRI is non-invasive, some patients especially the ones with metal objects in their body cannot be treated under MRI.

3.2 Pre-operative phase

The design of a robotic system requires a good knowledge of the working environment being the vascular network in this particular case. Such network with a total length close to 100,000 km per human adult consists of various types of blood vessels ranging in diameters and flow rates, while being located at various depths inside the body.

For imaging such environment, there is another critical challenge occurring in the pre-operative time frame that needs to be addressed. Indeed, presently and as mentioned previously, the best spatial resolution for imaging the blood vessels is ~0.2 mm and is achieved with an x-ray based technique known as Digital Subtraction Angiography (DSA) [17–19]. But DSA still have insufficient resolution in a clinical setting to image beyond the arteries such as the arterioles. Therefore, pre-operative tasks such as determining the proper path or trajectory in the form of successive waypoints in the vasculature is restricted to larger vessels such as the arteries.

As such, innovative approaches are needed. One particular approach [20] is the use of microparticles being released in an unknown microvascular network prior to be scanned by MRI several times during travel using the

Table 1 Imaging modalities for microrobotic-based interventions

Imaging modality	RT tracking	Min. size agent	Res.	Imaging	Inv.	Cost
US	Very High	Large	Low SNR	Soft Tissues	No	Very Low
PET	Medium	< 200 μm	Medium	Radio-isotopes	Yes	High
x-ray/CT	Very High	~200 μm	High (~200 μm)	Dense Structures and Bones	Yes	Medium
MRI	High to Low	< 200 μm	High (~500 μm)	Magnetic Structures and Soft Tissues	No	High

susceptibility artifact generated by the same microparticles. The information of the time discrete scans can be extracted and gathered to build up a 3D distribution of the local microvascular network. But at present, the approach needs further investigation to be suitable for such an application. For instance, determining the relative position of the microparticles within a voxel, although under investigation, is still a limiting factor among others that presently limits the usability of this technique. Nonetheless, although it appears that DSA may be the most suitable technique for narrower arteries, MRI-based novel approaches based on susceptibility artifacts could potentially prove to be more appropriate for vessels such as the arterioles but would likely be insufficient for the narrowest capillaries. This is due to the too weak susceptibility artifacts generated by the smaller (diameters of a few micrometers) particles needed to transit in such parts of the vascular network.

Therefore, since in vivo visualization of the microvasculature (especially when located deeply within the body) is presently not possible with any medical imaging modalities, closed-loop navigation control beyond the arterioles is unlikely. As such, other approaches must be investigated such as the use of self-propelled biological agents as discussed in more details later in this paper.

3.3 Post-operative phase

Not more can be said about post-operative imaging related to microrobotic interventions in the vasculature since assessing the work done including the targeting efficacy in drug delivery has the same imaging constraints as in the pre-operative phase. But with MRI, particularly in drug delivery interventions, the artifacts generated by the magnetic agents can be exploited to assess the targeting efficacy with a minimum number of agents as depicted in the example shown in Fig. 2b.

4 Actuation

4.1 Intra-operative imaging modality dependency

From the previous section, it becomes clear that the choice of an actuation mode [21] responsible for providing a force capable of influencing the displacement paths of navigable agents sufficiently to maintain them along a planned trajectory towards the final target would depend on the imaging modality used during the real-time closed-loop navigation phase. As such, although US could provide an adequate imaging modality with high sampling rates to robots or devices with an overall diameter of at least ~2 mm, the use of US would allow closed-loop interventions in the larger arteries only. X-ray or CT would expand the possible interventional area to arteries with microscale agents including robots and devices having a minimum diameter of ~0.2 mm. But to proceed beyond the arteries, MRI, although the real-time performance remains an issue, appears to be the only adequate imaging modality capable of detecting much smaller agents because of the presence of sufficiently large artifacts that allows their detections within the body.

Nonetheless, the choice of the medical imaging modality used in a real-time fashion during the intra-operative phase may put constraints on the choice of the actuation used for the navigable agent. This is especially true with MRI where the agent must be MRI-compatible while avoiding magnetic-based actuation unless such actuation mode exploits the magnetic fields of the MRI scanner. These modes of actuation for displacement purpose can be categorized as induced that are better suited for larger vessels, and the ones for the microvasculature, i.e., for higher and lower Reynolds number regimes respectively.

4.2 Actuation methods for larger diameter vessels

Presently, induced actuation methods considered for operation in the larger vessels of the vascular network rely on magnetism. In this cases, the performance in term of the actuation force induced (N) of can then expressed as

$$\overrightarrow{F} = R \cdot V_M \left(\overrightarrow{M} \cdot \nabla \right) \overrightarrow{B} \tag{3}$$

where R defined in the interval 0 to 1 represents the duty cycle of the pulling force being applied, i.e., the fraction of the time within a cycle where the pulling magnetic gradient responsible to induce a pulling force on the navigable agent is being applied. In (3), V_M is the total volume of magnetic material with a magnetization level $\boldsymbol{M}$ (A/m) embedded in the agent, with a magnetic flux density $\boldsymbol{B}$ (T). In (3), the gradient operator is expressed as

$$\nabla = \left[\frac{\partial}{\partial x} \frac{\partial}{\partial y} \frac{\partial}{\partial z} \right]^T \tag{4}$$

From (3), it can be observed that to decrease further the volume of the navigable agent, the magnetization level of the magnetic agent must be increased as close as possible to its magnetization saturation $\boldsymbol{M}_S$. Although this may not play a decisive decision in the development of future platforms, it is interesting to note that little progress has been made in improving the range of saturation magnetization of materials during the last 100 years [22]. Presently, the highest saturation magnetization is $M_S = 1.95 \times 10^6$ A/m is achieved by immersing a soft magnetic core made of iron-cobalt alloy containing 35 % cobalt in a field $B \geq 2.43$ T [22]. Compared to hard (permanent) Neodymium ($Nd_2Fe_{14}B$) magnet with a typical magnetization saturation expressed as remanence

M_r=1.3 T, soft magnetic materials are good candidates for the implementation of such navigable agents.

But systems relying only on one or more external permanent magnets such as the Niobe system [23] or a simpler system based on a magnet being mounted at the end of a robotic arm to position it around a patient [24], do not only provide insufficient magnetic flux density to bring such agents at magnetization saturation but are generally relatively slowed for changing the direction of the gradient field. Although acceptable for magnetically guided catheterization procedures, controlled capsule endoscopy, or particular microrobotic-based interventions performed in arteries such as plaque removal to name but only one example, the switching rate is typically not sufficient for other more demanding interventions such as the fast delivery of navigable therapeutic agents through more complex vascular networks. To increase the switching rate of the direction of the gradient, systems based on electrical coils or solenoids (cylindrical coils with a soft magnetic core) as a source of induced actuation as for the OctoMag system [25] are a better choice. But again, although such type of systems can generate relatively high magnetic gradients over a limited distance since such gradients decay rapidly with distance, B within the workspace can be relatively low. For the OctoMag system for example, considering a workspace of 4 cm^3, field gradients were up to 2 T/m but B=50 mT. Considering that the magnetization of soft magnetic materials with high magnetization saturation initially increases sharply with values of B just past zero with a significant reduction of the slope at much higher field magnitudes before reaching a plateau at magnetization saturation, increasing B beyond the values achieved by these systems would lead to a significant increase in the actuation force induced on the navigable agents. Without such increase of B, the workspace must be reduced which poses additional constraints on the depth at which the interventions can be performed within the body, and/or V_M must be increased to compensate for the loss in magnetization which would restrict interventions in larger diameter vessels only. Recently, a Magnetically Guided Capsule Endoscopy (MGCE) platform [26] has been jointly developed by Olympus Medical Systems Corp. and Siemens Healthcare. It has a B=100 mT within a larger workspace (equivalent to the human stomach) and was designed but considering the limit in the generation of magnetic fields, the system works only with larger objects (higher V_M).

Another approach consists in increasing the magnetization by exploiting the high homogeneous magnetic field (typically 1.5 T or 3 T) known as the B_0 field of a clinical MRI scanner [6, 27]. When immersed in such a field, magnetization saturation can be reached for all soft magnetic materials including soft magnetic cores achieving the highest magnetization such as iron-cobalt alloy containing 35 % cobalt at B=2.43 T using a 3 T scanner. Even the magnetization achieved within a 1.5 T scanner is far superior to other systems mentioned previously while being relatively close to the maximum achievable magnetization saturation. Another advantage is that the pulling force generated by the magnetic gradient is depth independent within the patient, i.e., that the method is as effective deeper under the surface of the skin as it is closer to the external source of the gradient field unlike the use of a gradient from an external magnet being applied in an area exempted of a high homogeneous magnetic field. This closed-loop navigation method using MRI as imaging modality as well as to provide the appropriate environment for such depth independent actuation in the form of a pulling force is the fundamental principle [27] of what has been referred to as Magnetic Resonance Navigation (MRN).

But MRN has also some limitations. The first limitation is the gradient field which is limited not only by technology-related issues but also by physiological constraints. Indeed, the slew rate dB/dt at higher gradients can pose a treat for the patient [28] since the mean threshold levels are 60 T/s for peripheral nerve sensation, 90 T/s for peripheral nerve pain, 900 T/s for respiratory system stimulation, and 3600 T/s for cardiac stimulation [29]. For clinical practices, the FDA guidelines suggest 0-20 T/s which limits gradient switching rates to a factor of 3 below the mean Peripheral Nerve Stimulation (PNS) level (> 20 T/s for first and second controlled modes limited by human ethical committee). As such, the typical operating range for MR-imaging is 45 T/s. This number suggests, using a maximum adequate rise time of 200 μs for MR-image sequencing, maximum gradient amplitudes of 90 mT m^{-1}. These gradients are relatively low and although compensated by a high magnetization level of the navigable agents, they still represent a limitation for achieving further miniaturization of the agents.

These facts suggest that the gradient field of a MRI scanner would need to be increased. Hence, the trend in the implementation of such upgraded MRI scanner capable of navigating smaller agents and referred to as a MRN system is to maximize the amplitude of the gradients while adjusting the slew rate within human limits (tolerances). But the implementation of these MRN platforms dedicated to human interventions is not an obvious task and brings additional challenges. Indeed, the strength of the gradient is determined by the amount of electrical current driven through each coil in an orthogonal assembly. Increasing a sustained gradient by approximately 10 times from typical clinical scanners to a maximum value of~±400 mT m^{-1} is very challenging but could technologically be feasible for human scale systems. Based on experimental results [8] using a smaller prototype designed for rabbit models, such systems would most likely be sufficient for the steering of agents with diameters as small as ~50 μm in arterioles under real human physiological conditions while being propelled using the blood flow.

But exploiting the blood flow for propulsion, which is required considering the limitations of all existing systems when operating in smaller diameter vessels located deeper in

the body, makes recovery of the agents impossible. This fact adds constraints on the synthesis of the navigable agents in term of cytotoxicity level, biodegradation, and immune system response, to name but a few factors. This may not be possible to conduct some types of interventions while being acceptable for others such as in drug delivery in cancer therapy for instance.

The B_o field inside a clinical MRI scanner also restricts operations to a maximum of three-degree-of-freedom (3-DOF) allowing 3D translational motion without rotation compared to 5-DOF for the OctoMag system for instance. This fact suggesting the use of shape-isotropic agents is due to the torque created by the B_o field aligned along the z-axis, i.e., along the longitudinal axis of the tunnel or bore of the MRI scanner. As such, the magnetic moment of the navigable agent or robot will experience a torque

$$\vec{T} = \vec{m} \times \vec{B} \tag{5}$$

Considering the orientation along the z-axis and the magnitude of the B_o field, we will have

$$\vec{m} = m_Z = V_M \cdot M_{SZ} \tag{6}$$

Although as mentioned earlier, such constraint is not critical for applications such as targeted delivery of therapeutics for cancer therapy for instance, it is not suitable for interventions such as some types of surgery that may require more DOF.

In an attempt to correct for such limitation in DOF while providing a higher magnetic flux to increase the magnetization level of the soft magnetic agents, another system has been proposed in [30]. It is referred to as the Electro Magnetic Actuation (EMA) system. The proposed system consists of four fixed coil pairs and one rotating coil pair. The coil system has 3 pairs of stationary Helmholtz coils, a pair of stationary Maxwell coils, plus a pair of rotating Maxwell coils. The Helmholtz coil pairs can magnetize and align the agent to the desired direction and the two pairs of Maxwell coil can generate the propulsion force. In addition, the Helmholtz coil pairs can rotate the agent about a desired axis. But looking at present state-of-the-art MRI scanner technology, especially in the difficulty in increasing the bore or tunnel inner diameter, suggests that providing a workspace with a diameter equivalent to the length of a patient instead of its width would call for a reduction of B in the working volume below the level typically used for MRN.

If rotation is not required, the primary choice of the induced actuation methods would be one with higher gradients but a lower field such as the OctoMag, or one with lower gradients but a higher field such as the MRN system. The choice may depend in great part to the magnetization curve of the navigable agent. For instance, for a given workspace, between a system providing 2 T/m and a maximum B=0.1 T versus a MRN system generating 0.4 T/m and a B=1.5 T, MRN will be advantageous in term of actuation alone used for inducing a pulling force if for the same navigable agent, the magnetization of the soft magnetic material at B=1.5 T is more than 5 times in this particular case, the value at B=0.1 T.

But other aspects must also be taken into account. For instance, since scaling a 0.4 T/m gradient coil to accommodate a human adult is already quite challenging, suggests that scaling with even higher gradients over a larger distance will be extremely difficult. Solutions leading to nonlinearity in the gradient fields could be introduced over a shorter distance and compensated with more complex algorithms to ease the implementation. Furthermore, although the magnitude of the magnetic field B does not pose a treat for the patient, this is not necessary true for the slew rate dB/dt at higher gradients. For instance, when operating at the typical operating range for MR-imaging of 45 T/s, a 2 T/m versus a 0.4 T/m gradient will limit the maximum real-time operating switching frequency to 11 Hz and 56 Hz respectively. A higher switching frequency such as for MRN based on a higher field with lower gradients may prove essential in more complex vascular networks characterized with relatively short distances between vessels bifurcations and operating within a high blood flow rate.

Besides these safety issues that may impact the maximum operating frequency of the system, the variable R in Eq. 3 must also be taken into account. Indeed, overheat caused by cooling limitation of the coils especially the ones generating high gradients over a large workspace may impose a reduction of the duty cycle for switching such gradients at relatively high frequency for relatively long interventions. For MRN, the advantages of having MRI as an image modality during the intra-operative phase is paid unlike other imaging modalities including x-ray, by a reduction of R since MR-imaging and MR-actuation cannot be performed simultaneously.

Other variances are possible including the use of more complex agents. For instance, a travelling-based propulsion method has been proposed in [31] that also operate inside a MRI scanner. RF coils of an MRI system are used to transmit power wirelessly to electronics embedded in the agent or microrobot which in turn distribute the electrical current to individual coils to induce a wave motion. Preliminary data suggest that the miniaturization of such propelled system will be a limiting factor for intervention in the vascular network. Other mechatronic and more complex implementations with onboard actuation mechanisms including piezoelectric ultrasonic micro-motor [32] have also been proposed and as the preceding example, miniaturization of these more complex agents is among the most important limiting factors for operation in the vascular network.

Although not exhaustive, Table 2 compares some of the fundamental actuation systems that that have been proposed or could be adapted for operations in larger blood vessels

such as the arteries and potentially in the arterioles. These systems include a single magnet attached to a robotic arm that can be positioned around the patient and the Niobe system (designated "Permanent Magnets" in Table 2), an OctoMag type platform or a variance that could be theoretically scaled for human interventions, the MGCE and the EMA platforms mentioned previously, the MRN system and finally, several more complex agents (designed "Agent" in Table 2) that have some form of onboard actuation mechanisms relying on mechatronics, piezo-actuation, etc.

As depicted in Table 2, the MGCE, EMA and the complex agents are restricted to interventions in larger arteries (few mm in diameter). This is due to the low field and gradients of the MGCE and EMA systems and the limit in miniaturization of the more complex agents. MRN can reach the arterioles because of the high field and sufficiently high gradients as validated experimentally in [8] for the TMMC and the possibility of closed-loop navigation by detecting smaller magnetic agents using MRI as imaging modality. For an OctoMag type platform, PET as for MRN using PET in PET-MRI technology could be theoretically used in a closed-loop fashion beyond the arteries if instead of x-ray to detect smaller agents. Using PET would bring some disadvantages as identified in Table 1 including the invasiveness of the approach, a much lower precision compared to MRI, and a slower acquisition rate. Unlike for MRN, navigation in the arterioles using an OctoMag type platform has not been yet validated experimentally.

For the permanent magnets platforms, the time required for repositioning the magnet or magnets to change the direction of the gradient is an important limiting factor for interventions passed the arteries. MRN is also the only method that can exploit the full magnetization of soft magnetic cores embedded in the navigable agents, allowing for the use of lower gradients and hence, facilitating scaling while allowing faster switching frequency or changes in the gradients within safety constraints for the patient. Furthermore, since the agent remains at the constant magnetization saturation level within the entire workspace, linear gradients surrounding the patients become depth independent ("No Decay" in Table 2) within the body.

4.3 Actuation methods in the microvasculature

Actuation methods in the microvasculature must be efficient in low Reynolds number regime while avoiding the miniaturization limitation of the navigable agent imposed by magnetic induced pulling force that restricts interventions passed the arterioles.

Therefore, other methods could be envisioned and magnetic actuation using a uniform rotating magnetic field to induce a torque along the helical axis of artificial micro-swimmers [33, 34] or Artificial Bacterial Flagella (ABF) [35] could be investigated further for such applications. ABF consists of a micro-helical propeller attached to a ferromagnetic bead acting as the head. Such artificial helical swimmer can have a size comparable to a natural flagellated bacterium and as the latter, flagellated propulsion is known to be very effective for displacement in low Reynolds number regime. For ABF, the amplitude of the magnetic field to generate a torque on the ferromagnetic bead acting as the head is much lower than the one needed to generate a pulling force, allowing such an agent to be miniaturized further and to have an overall diameter of ~2 μm, allowing potential navigation in the tiniest capillaries (min. diam. of ~4 μm) found in humans. But some challenges or requirements must be met before ABF can be applicable in this case. First, such ABF would have to meet biocompatibility requirements since recovery will be unlikely. But the most challenging issue such as for reaching a tumor for delivering drug for instance would be for these ABFs to transit through the complex and chaotic capillary network surrounding the tumor without external closed-loop navigation control since such blood vessels cannot be visualized in vivo by any existing medical imaging modalities. This issue would apply to all artificial and synthetic implementations including chemically propelled agents where the latter may bring an additional constraint related to the issue of specific chemicals in the blood. Furthermore, since an ABF is anisotropic in shape, it cannot be placed inside the high homogeneously field of a MRI scanner during the intra-operative phase because of the imposed directional torque Eq. 5 along the z-axis of the scanner.

Table 2 Actuation systems for interventions in larger vessels

Actuation system	Vessel types	B field	Gradients	Distance	Switching rate	DOF	Imaging modality
Permanent magnets	Arteries	Low	Very High	Decay	Slow	High but Slow	All except MRI
OctoMag type	Arteries+(Arterioles)	Low	Very High	Decay	Fast	5-DOF	All except MRI
MGCE EMA	Large Arteries	Low	Low	Decay	Fast	5-DOF	All except MRI
MRN	Arteries+Arterioles	Very High	Low to Medium	No Decay	Fast	3-DOF (Transl.)	MRI (PET-MRI)
Agent	Large Arteries	NA	NA	NA	NA	High	All+(MRI)

NA Not Applicable

Besides artificial structures, another approach relies on harvesting self-propelled agents such as natural flagellated bacteria carrying a load and being directionally controlled towards a pre-defined target as initially reported in [36] using Magnetotactic Bacteria (MTB) [37] as the preferred choice. Indeed, MTB has a chain of magnetite nanoparticles (known as magnetosomes) embedded in the cell. Such chain acts like a miniature magnetic compass needle [38], also referred to as magnetotaxis [39]. Magnetotaxis directional control is then achieved by inducing a directional torque from a relatively low magnitude magnetic field since the bacteria respond to the geomagnetic field. Among various species of MTBs, the MC-1 bacterium has been of special interest for operation in the microvasculature because it has not only a rounded cell with an ideal diameter between 1 and 2 μm but it also has the highest thrust force known so far and which has been measured in the range of ~4.0 to 4.7 pN [40]. Such thrust allows the bacterium to swim between ~100-150 body (cell) lengths per second.

Another advantage of such a natural or biological agent that can act and execute tasks in a similar manner as the ones envisioned for a futuristic microrobot, is the self-reproducibility achieved during cultivation that reduces significantly implementation cost and complexity. Such bacterium can also be functionalized by attaching therapeutics using binding techniques such as the use of monoclonal antibodies to self-assemble hybrid agents. Such a hybrid agent is already under development for the case of colorectal cancer in humans [41].

But more interesting is the fact that we know from experiments conducted in animal models that MTB can be very effective for transiting through complex capillary networks without real-time closed-loop navigation control. Experiments also showed their ability to penetrate deep in tumors when directed with a special new platform referred to as a magnetotaxis system [42]. Such new microrobotic platform not only offers the capability to direct these MTBs in a targeted region in a 3D space such as inside a tumor, but it also offers the capability to force these MTBs to aggregate. Such capabilities have been proven to be essential for effective targeting and delivery of specific amount of therapeutics.

But some constraints are also associated with the use of these MTB-tagged agents. For the non-pathogenic MC-1 bacteria for instance, the thrust force and hence the swimming velocity decreases as soon as the bacteria are exposed to the body temperature and will be null after ~40 min. This means that unlike an artificial or a synthetic agent, MC-1 bacterial agents must reach the tumor before the thrust force becomes ineffective to reach deeper in the tumor. One strategy is to inject MTB-tagged agents closer to the tumor which is as mentioned earlier, being investigated in the case of rectal or colorectal cancer. But for other types of cancers, this is not an option and such injections must be done in the arteries. This suggests the use of special MRN-compatible microcarriers to transport at high velocities, the MTB-tagged agents closer to the microvasculature prior to be released [43]. Although such microcarriers carrying living MC-1 bacteria have already be synthesized [44], additional work needs to be done before they can be evaluated in vivo.

Other issues must also be evaluated such as the cytotoxicity level and immune system response to name but only two. Presently, preliminary data show encouraging results for the MC-1 bacterium but more tests are necessary. But although preliminary data suggest that MTBs will not be initially recognized by the immune system, immune system response is likely to occur shortly and most likely within a few days after the first injection. Although the exact delay for the immune system to respond is still unknown but presently under investigation, it is most likely that repetitive interventions over a relatively long period of time would not be possible. Therefore, assessing the targeting efficacy and hence the predicted therapeutic outcome by observing tumor regression alone after several weeks will probably not be an option. This fact emphasizes the need to assess the targeting efficacy in term of quantity and distribution of the MTB-tagged agents as soon as possible after the completion of the intra-operative phase. This brings additional challenges in localizing such MTB beyond MR imaging. Although it was demonstrated that magnetosomes embedded in MTB can produce positive MRI contrast [45], the quantity and density of the colony must be very high to be detectable. Therefore, there will be a need to increase the detection sensibility by introducing extremely small markers such as radioisotopes attached to such agents that could be detected by a sensitive imaging modality such as PET for instance.

Knowing that the position of a target such as tumor can be gathered during the pre-operative phase since it can be visualized with MRI, magnetotaxis where a platform is used to indicate the position of the target to MTB-tagged agents within a relatively large workspace, is certainly an interesting and valuable concept. But instead of using a directional magnetic field to influence the swimming direction of the bacteria towards the target, the directional motion of bacterial agents could theoretically be influenced by a specific attractant located at the target. For instance, anaerobic bacteria have been investigated as tumor-targeting vectors [46] based on initial observations [47–49]. Anaerobic bacteria are indeed of special interest for such type of treatments since they are attracted to the oxygen starved areas of tumors. But studies showed that only a fraction of bacteria reached the tumor after a systemic injection. Such approach may as in chemotherapy, increase systemic circulation of toxic therapeutics affecting healthy organs while increasing secondary toxicity for the patient. The major problem with the use of an attractant is the distance at which such attractant can be detected by the bacteria. So, for other bacterial agents being investigated and exploiting specific taxis such

as chemotaxis (or another taxis) such as in [50–52], the main drawback is the range at which the attractant can be detected from the source and if the source can produce an attractant being recognized by the same bacteria. A review of bacterial microsystems and microrobots can be found in [53].

5 Conclusions

Microrobotics for operations in the vascular network offers huge opportunities in future targeted medical interventions. But to exploit its full potential, several challenges need to be addressed within a highly interdisciplinary environment. In this paper, these major critical challenges have been identified and briefly described.

Despite these challenges, the field of micro nanorobotics for operations in the vascular network is progressing at a relatively fast pace and the interdisciplinary nature of this specialized field of robotics if mastered adequately, should contribute to push further the field to provide new solutions that would most likely lead to substantial great outcomes for the patients.

Acknowledgment The author acknowledges the financial support from the Research Chair of École Polytechnique in nanorobotics and in part from a Discovery grant from the National Sciences and Engineering Research Council of Canada (NSERC).

References

1. Jain KK (2005) Editorial: targeted drug delivery for cancer. Technology in Cancer Treatment 4(4):311–313
2. Nguyen KT (2011) Targeted nanoparticles for cancer therapy: promises and challenges. J Nanomedicine and Nanotechnology 2 (5)
3. Pouponneau P, Leroux J-C, Martel S (2009) Magnetic nanoparticles encapsulated into biodegradable microparticles steered with an upgraded magnetic resonance imaging system for tumor chemoembolization. Biomaterials 30(31):6327–6332
4. Olamaei N, Cheriet F, Martel S (2011) Accurate positioning of magnetic microparticles beyond the spatial resolution of clinical MRI scanners using susceptibility artifacts. In Proc. 33rd Annual Int. Conf. of the IEEE Eng. in Medicine and Biology Society (EMBC), Boston, USA
5. Olamaei N, Beaudoin G, Cheriet G, Martel S (2010) MRI visualization of a single 15 μm navigable imaging agent and future microrobot. 32nd Annual International Conference of the IEEE Engineering in Medicine and Biology Society (EMBC), Buenos Aires, Argentina
6. Martel S, Mathieu J-B, Felfoul O, Chanu A, Aboussouan É, Tamaz S, Pouponneau P, Beaudoin G, Soulez G, Yahia L'H, Mankiewicz M (2007) Automatic navigation of an untethered device in the artery of a living animal using a conventional clinical magnetic resonance imaging system. Appl Phys Lett 90:114105
7. Felfoul O, Mathieu J-B, Beaudoin G, Martel S (2008) MR-tracking based on magnetic signature selective excitation. IEEE Trans on Medical Imaging 27(1):28–35
8. Pouponneau P, Leroux J-C, Soulez G, Gaboury L, Martel S (2011) Co-encapsulation of magnetic nanoparticles and doxorubicin into biodegradable microcarriers for deep tissue targeting by vascular MRI navigation. Biomaterials 32(13):3481–3486
9. Mathieu J-B, Martel S (2009) Aggregation of magnetic microparticles in the context of targeted therapies actuated by a magnetic resonance imaging system. J Appl Phys 106: 044904-1 to 7
10. Mathieu J-B, Martel S (2010) MRI Steering of aggregating magnetic microparticles for enhanced therapeutic efficacy in cancer targeting. Magn Reson Med 63:1336–1345
11. Beyer T, Towsend DW, Brun T, Kinahan PE, Charron M, Roddy R, Jerin J, Young J, Byars L, Nutt R (2000) A combined PET/CT scanner for clinical oncology. J Nucl Med 41(8):1369–1379
12. Seemann MD (2005) Whole-body PET/MRI: the future in oncological imaging. Technol Cancer Res Treat 4(5):577–582
13. Judenhofer MS et al (2008) Simultaneous PET-MRI: a new approach for functional and morphological imaging. Nat Med 14:459–465
14. Pichler BJ, Kolb A, Nagele T, Schlemmer H-P (2010) PET/MRI: paving the way for the next generation of clinical multimodality imaging applications. J Nucl Med 51(3):333–336
15. Martin A, Weber O, Saloner D, Higashida R, Wilson M, Saaed M, Higgins C (2002) Application of MR technology to endovascular interventions in an XMR Suite. Medicamundi 46(3):28–34
16. Belharet K, Folio D, Ferreira A (2010) Endovascular navigation of a ferromagnetic microrobot using MRI-based predictive control. In Proc. IEEE/RSJ Int. Conf. on Intelligent Robots and Systems (IROS), Taipei, Taiwan, pp 2804-2809
17. Brody WR (1982) Digital subtraction angiography. IEEE Trans Nuclear Science 29(3):1176–1180
18. Tobis JM, Nalcioglu O, Henry WL (1983) Digital subtraction angiography. Chest 84(1):68–75
19. Weinstein PR (1983) Digital subtraction angiography. Clin Neurosurg 31:90–106
20. Olamai N, Cheriet F, Martel S (2012) 3D reconstruction of microvasculature in MRI using magnetic microparticles. In Proc. 11th Int. Conf. on Information Sciences, Signal Processing and their Applications, Montréal
21. Nelson BJ, Kaliakatsos IK, Abbott JJ (2010) Microrobots for minimally invasive medicine. Annu Rev Biomed Eng. pp 55-85
22. Jiles DC (2003) Recent advances and future directions in magnetic materials. Acta Mater 51:5907–5939
23. Carpi F, Pappone C (2009) Stereotaxis Niobe magnetic navigation system for endocardial catheter ablation and gastrointestinal capsule endoscopy. Expert Rev Med Devices 6(5):487–498
24. Valdalstri P, Sinibaldi E, Caccavaro S, Tortora G, Menciassi A, Dario P (2011) A novel magnetic actuation system for miniature swimming robots. IEEE Trans Robot 27(4):769–779
25. Kummer MP, Abbott JJ, Kratochvil BE, Borer R, Sengul A, Nelson BJ (2010) OctoMag: an electromagnetic system for 5-DOF wireless micromanipulation. IEEE Trans Robot 26(6): 1006–1017
26. Keller H, Juloski A, Kawano H, Bechtold M, Kimura A, Takizawa H, Kuth R (2012) Method for navigation and control of a magnetically guided capsule endoscope in the human stomach. The 4th IEEE RAS/EMBS Int. Conf. on Biomedical Robotics and Biomechatronics (BioRob), Roma, Italy, pp 859-865
27. Mathieu J-B, Beaudoin G, Martel S (2006) Method of propulsion of a ferromagnetic core in the cardiovascular system through magnetic gradients generated by an MRI system. IEEE Trans Biomed Eng 53(2):292–299
28. Schaefer DJ, Bourland JD, Nyenhuis JA (2000) Review of patient safety in time-varying gradient fields. J Magn Reson Imaging 12:20–29
29. Price RR (1999) The AAPM/RSNA physics tutorial for residents: MR imaging safety considerations. Radiographics 19:1641–1651

30. Yu C, Kim J, Choi H, Choi J, Jeong S, Cha K, Park J, Park S (2010) Novel electromagnetic actuation system for three-dimensional locomotion and drilling of intravascular microrobot. Sensors and Actuators A: Physical 161(1–2):297–304
31. Kosa G, Jakab P, Szekely G, Hata N (2012) MRI driven magnetic microswimmers. Biomed Microdevices 14(1):165–178
32. Watson B, Friend J, Yeo L (2010) Modelling and testing of a piezoelectric ultrasonic micro-motor suitable for in vivo microrobotic applications. J Micromech Microeng. 20(115018):16
33. Honda T, Arai KI, Ishiyama K (1996) Micro swimming mechanisms propelled by external magnetic fields. IEEE Trans Magn 32 (5):5085–5087
34. Ghosh A, Fisher P (2009) Controlled propulsion of artificial magnetic nanostructured propellers. Nano Lett 9(6):2243–2245
35. Zhang L, Abbott JJ, Dong LX, Kratochvil BE, Bell DJ, Nelson BJ (2009) Artificial bacterial flagella: fabrication and magnetic control. Appl Phys Lett 94:064107
36. Martel S, Tremblay C, Ngakeng S, Langlois G (2006) Controlled manipulation and actuation of micro-objects with magnetotactic bacteria. Appl Phys Lett 89:233804–6
37. Blakemore RP (1975) Magnetotactic bacteria. Science 190:377–379
38. Frankel RB, Blakemore RP (1980) Navigational compass in magnetic bacteria. J Magn Magn Mater 15–18(3):1562–1564
39. Debarros H, Esquivel DMS, Farina M (1990) Magnetotaxis. Sci Progr 74:347–359
40. Martel S, Mohammadi M, Felfoul O, Lu Z, Pouponneau P (2009) Flagellated magnetotactic bacteria as controlled MRI-trackable propulsion and steering systems for medical nanorobots operating in the human microvasculature. IJRR 28(4):571–582
41. Martel S et al (2011) SN-38 (ot 5-FU) drug encapsulation in liposomes transported by magnetotactic bacteria for localized colorectal cancer treatment. Quebec Consortium for Drug Discovery (CQDM)
42. Felfoul O, Mohammadi M, Gaboury L, Martel S (2011) Tumor targeting by computer controlled guidance of magnetotactic bacteria acting like autonomous microrobots. In Proc. IEEE/RSJ Int. Conf. on Intelligent Robots and Systems (IROS*)*, San Francisco, USA
43. Martel S, Felfoul O, Mathieu J-B, Chanu A, Tamaz S, Mohammadi M, Mankiewicz M, Tabatabaei N (2009) MRI-based nanorobotic platform for the control of magnetic nanoparticles and flagellated bacteria for target interventions in human capillaries. (IJRR), Special Issue on Medical Robotics 28(9):1169–1182
44. Afkhami F, Taherkhani S Mohammadi M, Martel S (2011) Encapsulation of magnetotactic bacteria for targeted controlled delivery of anticancer agents for tumor therapy. In Proc. of the 33rd Annual Int, Conf. of the IEEE Eng. in Medicine and Biology Society (EMBC), Boston, USA
45. Benoit MR et al (2009) Visualizing implanted tumors in mice with magnetic resosance imaging using magnetotactic bacteria, Clin Cancer Res 15(16):5170–5177
46. Pawelek JM, Low KB, Bermudes D (2003) Bacteria as tumour-targeting vectors. Lancet Oncol 4:548–56
47. Coley B (1891) Contribution to the knowledge of sarcoma. Ann Surg 14:199–220
48. Nauts HC, Swift WE, Coley BL (1946) The treatment of malignant tumors by bacterial toxins as developed by the late William B. Coley, MD, reviewed in the light of modern research. Cancer Res 6:205–216
49. Willis AT (1960) Anaerobic bacteriology in clinical medicine. London: Butterworth, p 40
50. Kim D, Liu A, Sitti M (2011) Chemotactic behavior and dynamics of bacteria propelled microbeads. IEEE/RSJ Int. Conf. in Intelligent Robots and Systems, San Francisco, USA
51. Steager E, Kim C, Patel J, Bith S, Naik C, Reber L, Kim M (2007) Control of microfabricated stuctures powered by flagellated bacteria using phototaxis. Appl Phys Lett 90:263901–3
52. Nogowa K, Kojima M, Nakajima M, Homma M, Arai F, Fukada T (2011) Smart manipulation of multiple bacteria-driven microobjects based on baceria autonomous movement. IEEE Int. Conf. on Intelligent Robots and Systems (IROS), pp 1693-1698
53. Martel S (2012) Bacterial microsystems and microrobots. Biomed Microdevices, doi:10.1007/s10544-012-9696-x, printed online 9 Sept. 2012, accepted for printed publication